2.C:3.A *Nuclear Physics* A173 (1971) 177—206;

DE-EXCITATION OF THE ^{61}Cu COMPOUND NUCLEUS VIA PHOTON EMISSION FROM PROTON AND NEUTRON UNBOUND STATES

EDWARD J. HOFFMAN † and DEMETRIOS G. SARANTITES
Chemistry Department, Washington University, St. Louis, Missouri 63130, USA ††

Received 9 March 1971
(Revised 19 May 1971)

Abstract: The relative yields to many levels in ^{61}Cu and ^{60}Ni populated via the ^{58}Ni(^{4}He, pγ)^{61}Cu and the ^{58}Ni(^{4}He, 2pγ)^{60}Ni reactions were measured at 15.0, 18.0, 20.0 and 22.0 MeV of ^{4}He^{++} bombardment energies. The relative independent yields for the population of many individual levels in ^{61}Cu, defined to include all unobserved cascades, were measured as a function of excitation energy in the ^{61}Cu compound nucleus for each of the above bombardment energies. The experiment consisted of a two-parameter measurement of the γ-rays characteristic of ^{61}Cu or of ^{60}Ni observed in coincidence with protons of measured energy. The relative cross sections are found to peak at 3–7 MeV above the proton separation energy for many levels in ^{61}Cu. The reported results present direct evidence for photon emission from proton and neutron unbound states. The energy dependence of photon emission in competition with proton emission and with neutron emission at the higher bombardment energies is quantitatively determined for many levels in ^{61}Cu with known J^π values. The effect of the average angular momentum of the compound nucleus on the photon versus proton emission is reflected on the observed change of the integrated independent yields and on the position of the maximum of the independent yield curve with excitation energy for states of different J^π value when the bombardment energy is increased. The relative independent yields for the first six excited states in ^{60}Ni were also measured as a function of the observed proton energy in coincidence with the γ-ray de-exciting the level in question. The ratios of the integrated independent yields for many pairs of levels in ^{61}Cu and ^{60}Ni populated in the (^{4}He, pγ) and (^{4}He, 2pγ) reactions were also obtained. The results of these experiments are consistent with the predictions of the compound statistical theory for nuclear reactions. The present results demonstrate that photon emission in competition with nucleon emission plays a dominant role in the outcome of reactions induced by ^{4}He^{++} for energies where multiple nucleon emission occurs.

E NUCLEAR REACTIONS ^{58}Ni(^{4}He, pγ), ^{58}Ni(^{4}He, 2pγ), ^{58}Ni(^{4}He, pnγ), $E = 15$–22 MeV; measured $\sigma(E; E_p, E_\gamma)$ and pγ coinc., p$\gamma(\theta)$, $\gamma N(E_p)$ and $I_\gamma(E^*)$ yield for independent formation for levels in ^{61}Cu, ^{60}Ni and ^{60}Cu; deduced dependence on excitation energy of photon emission from proton and neutron unbound states ^{61}Cu levels deduced J, π. J-values. Enriched targets; Ge(Li), NaI-Ge(Li) anti-Compton spectrometers, Si(Li) and Si surface-barrier annular detectors, $E \cdot \Delta E$ Si(Li) telescope.

1. Introduction

In recent years attention was drawn by several investigators to the role of angular momentum on the outcome of a large class of nuclear reactions induced by medium

† Present address: Bartol Research Laboratory, Swarthmore, Pennsylvania.

†† This work was supported in part by the US Atomic Energy Commission under Contract NOS. At(11-1)-1530 and AT(11-1)-1760.

and high-energy $^4He^{++}$ or heavy ions and assumed to proceed via the formation and decay of a compound nucleus [see for example refs. [1-5])]. Further, it was realized that the γ-ray emission plays a significant role in the nuclear de-excitation process. Experimentally, Mollenauer [6]) measured the yield of γ-rays from ^{12}C-ion induced reactions on Te and V and found the γ-rays emitted to be quadrupole in character. Alexander and Simonoff [4]) measured by recoil techniques the average energy and angular momentum removed by neutrons and by photons from Dy compound nuclei and report that 2–4 $\hbar$ units of angular momentum are removed by the first neutron and that each average individual photon removes, on the average, 1.8 ± 0.6 $\hbar$ units of angular momentum. In an analysis of excitation functions and isomer yield ratios in the $^{107}Ag(^4He, xn)$ reactions Sarantites and Pate [1]) and Sarantites [2]) pointed out that γ-ray emission played a dominant role in the outcome of the so-called evaporation cascade. In fact, using the statistical model with the proper dependence of the emission probability on angular momentum [1, 2]) and realistic parameters which reproduced both the measured excitation functions and the isomer ratios, the last mentioned authors pointed out that at the higher bombardment energies a large fraction of the (^4He, n) reaction cross section originated from cascades in which γ-ray emission dominated neutron emission for excitation energies as high as 3 MeV above neutron separation energy. At about the same time Grover and Gilat [3]) reported similar results of calculations based on the compound statistical theory. These authors pointed out that the levels of the highest angular momentum for a given excitation energy, which they termed the "yrast levels", played a significant role in the de-excitation process. Grover and Gilat [3]) further point out that there is a region in the $E-J$ phase-space diagram defined by the line of the yrast levels and a $k_\gamma = 0.5$ line [3]), in which γ-ray emission dominates against neutron emission.

In the past few years a considerable number of studies have been reported on the γ-rays in the de-excitation of the product nuclei following compound-nucleus reactions induced by projectiles ranging from ^4He to ^{40}Ar ions. Much of this work has been summarized by Newton *et al.* [7]) who have proposed a model for the explanation of the mechanism for the population of the members of the ground state rotational band (g.s.b.) in the deformed nuclei from cascades through the yrast levels. Considerable experimental information has been accumulated [7]) from such (HI, $xn\gamma$) reaction studies about the position and population of many levels which are members of the g.s.b. and which for low excitation energy play the role of yrast levels. More direct experimental evidence, however, on the region of excitation energy for which photon emission predominates over nucleon emission has not yet been reported.

During the preparation of this manuscript Cohen *et al.* [8]) reported results of a (p, np) coincidence study on ^{90}Zr and ^{112}Sn from which they deduce that γ-ray emission in competition with proton emission appears to be unimportant above 3.3 MeV in the reaction on ^{90}Zr and above 4.3 MeV in the reaction on ^{112}Sn.

In this paper we present results of the measurement of the relative magnitude of photon emission from proton and neutron unbound states in a ^{61}Cu compound

nucleus. The relative independent yields for the population of many levels in ^{61}Cu and ^{60}Ni via the ^{58}Ni(^{4}He, pγ) or ^{58}Ni(^{4}He, 2pγ) reactions were measured at four bombardment energies of 15, 18, 20 and 22 MeV. By measuring the energy of the protons emitted in coincidence with characteristic γ-rays known to belong to ^{61}Cu it was possible to determine the excitation energy from which each γ-ray cascade initiated. It is shown that γ-ray emission is predominant for excitation energies up to 3 or 7 MeV above the proton separation energy, depending on the bombardment energy. The independent yields for the population of the first six excited states in ^{60}Ni by the (^{4}He, 2p) reaction were also obtained. The ratios of the energy integrated independent yields for many pairs of levels in ^{61}Cu and ^{60}Ni populated in these reactions are presented and their change with bombardment energy is discussed in terms of the compound-statistical theory for nuclear reactions.

2. Experimental procedures

2.1. THE CYCLOTRON FACILITY

In these experiments the external beam facility of the Washington University cyclotron was used to provide the 15.0–22.0 MeV $^{4}He^{++}$ beams required. This facility has been described in some detail elsewhere [9]). The variable energy feature of our cyclotron was utilized to provide the 15.0, 18.0, 20.0 and 22.0 MeV $^{4}He^{++}$ beams employed in most of these experiments. For the coincidence and the singles experiments beam currents of 1–5 and 100–200 nA were used, respectively.

2.2. SCATTERING CHAMBERS AND CHARGED-PARTICLE COUNTING

Three different target mounting assemblies and scattering chambers were used in this work and these have been described in subsect. 2.2 of ref. [10]). Briefly, these consisted of (i) a miniature scattering chamber which was used for the pγ coincidence angular correlation measurements, (ii) a precision 110 cm scattering chamber, which was used to obtain $(E \cdot \Delta E)$ mass-identified proton and α-particle spectra, and (iii) a large solid angle assembly, which was used for the coincidence yield measurements with a Ge(Li) detector placed at 90° to the beam direction.

For singles charged particle counting a $(E \cdot \Delta E)$ mass identifying telescope was used. This consisted of a 1.0 mm × 1.0 cm^2 Si(Li) detector for the total absorption detector and a 0.100 mm × 1.0 cm^2 totally depleted Si(Li) detector.

For charged-particle counting in the pγ coincidence experiments an annular surface-barrier detector with an active area of 300 mm^2 and depletion depth of 1.0 mm was employed. This detector system had a resolution of 40 keV for 5.808 MeV α-particles from a ^{244}Cm source. The beam resolution was slightly over 1 % of the incident energy and the overall proton resolution including target thickness and kinematic spread varied between 300 and 450 keV for the energy range of 15 and 22 MeV of bombardment energy.

2.3. GAMMA-RAY COUNTING

For singles γ-ray counting a 29 cm^2 Ge(Li) detector with a resolution of 2.8 keV (FWHM) for the 1332 keV line of ^{60}Co was employed in an anti-Compton arrangement. The performance and calibration of this spectrometer have been described in some detail in ref. [9]). This spectrometer and its Pb shield were mounted on an angular correlation table. For singles γ-ray energy measurements the spectrometer was placed at 90° with respect to the beam to minimize distortion of the γ-peaks due to Doppler shift and broadening.

In order to determine the contribution from "delayed" γ-rays due to radioactivity build-up in the target, several pulsed experiments were performed [see ref. [10])].

For the pγ coincidence experiments a 40.8 cm^3 Ge(Li) with an active area of 10.7 cm^2 and a length of 3.80 cm was employed. This detector had a typical resolution of 2.3 keV and a peak-to-Compton edge ratio of 25 : 1 for the 1332 keV line of ^{60}Co. This detector was also mounted on another angular correlation table and could be rotated between 0°–90° with respect to the beam direction outside the miniature scattering chamber. This arrangement was used in the measurement of pγ coincidence correlations at 20 MeV.

For the energies employed in these experiments the period between beam bursts varied from 106–129 ns while the width of each burst was $\approx$4 ns. For the energy range of 15–22 MeV of ^{4}He^{++} employed in these experiments, the prominent reactions are (^{4}He, p), (^{4}He, 2p), (^{4}He, n), (^{4}He, pn), (^{4}He, αp) and (^{4}He, αn) with Q-values at -3.108, -7.908, -9.295, -14.704, -8.178 and -12.195 MeV, respectively. Of these the (^{4}He, p), (^{4}He, 2p) and (^{4}He, pn) reactions contributed to the desired pγ coincidence events, while the (^{4}He, nγ) and the γ-rays from the decay of ^{61}Zn, ^{61}Cu and ^{60}Ni produced during bombardment contributed to the random events. Under these conditions and with the 300 cm^2 Si detector at a distance of 1.3 cm from the target and with the Ge(Li) detector at 2.5 cm from the target, it was possible to accumulate data at a total coincidence rate between 100–300 c/sec. In all the experiments the rate of random coincidence events was kept below 5 % of the total rate. It should be noted that the prompt coincidence peak had a time width of $\approx$70 ns at $\frac{1}{10}$ height, and this allowed the rejection of random events from neighboring satellite beam bursts.

For pulse-height analysis a Nuclear Data, Inc. Model No. 161 4096-channel two-parameter pulse-height analyzer was used. This analyzer was equipped with a buffer-tape and a read-search control unit, coupled with an IMB computer compatible magnetic tape drive. This analyzer with 18 binary bit related address capability was employed in all the pγ coincidence and correlation experiments.

3. Experimental results

The analysis of the results presented in this study depends on the detailed knowledge of the level scheme and of the decay properties of the levels in ^{61}Cu. A detailed study of this decay scheme was given in ref. [10]).

3.1. SINGLES PARTICLES AND γ-RAY MEASUREMENTS

In order to determine the number of α-particles emitted at the backward angles relative to the number of protons, spectra of these two types of particles were recorded simultaneously be means of $(E \cdot \Delta E)$ mass identification and proper routing of the pulse-height analyzer. Typical proton and alpha particle spectra are shown in fig. 1

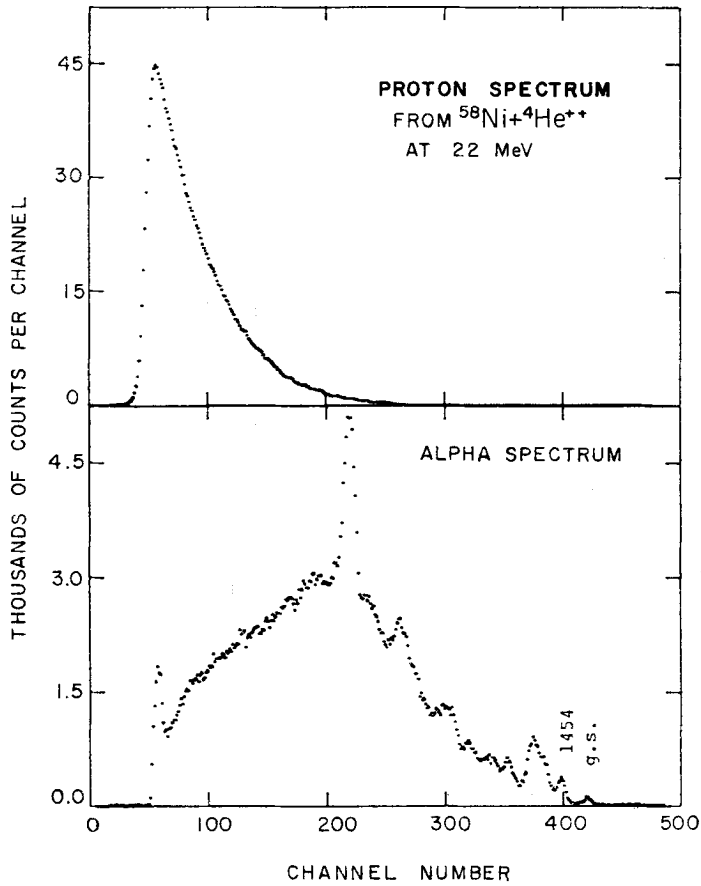

Fig. 1. Proton and α-particle spectra obtained with the $(E \cdot \Delta E)$ detector telescope at 154° from ^{58}Ni+^{4}He^{++} at 22.0 MeV of bombardment energy. At this energy the protons from the (^{4}He, p) reaction show a continuum distribution and the number of protons emitted is considerably larger than that of α-particles.

and they were taken at 22 MeV bombardment energy with the $(E \cdot \Delta E)$ detector telescope at an angle of 154°, which is close to the average solid angle of the annular detector used in the pγ coincidence experiments. From such spectra taken at various ^{4}He^{++} bombardment energies between 15 and 22 MeV, it was found that the fraction of α-particles detected at 154° progressively diminished with increasing bombardment energy. Since good energy resolution was achieved for the γ-rays, the competing

(^{4}He, $\alpha'\gamma$), (^{4}He, $\alpha p\gamma$) and (^{4}He, $\alpha n\gamma$) reactions, which were shown to have lower cross sections, did not interfere with the $p\gamma$ coincidence experiments.

Singles spectra of the prompt γ-rays from the $^4He^{++}$ induced reactions on ^{58}Ni at 15, 18, 20 and 22 MeV were taken with the Compton-suppression spectrometer under a pulsed beam operation. This allowed us to determine the spectra of the delayed γ-rays from the radioactivity produced in the target. A typical spectrum of the γ-rays emitted at 90° in the $^{58}Ni + ^4He^{++}$ reaction at 20.0 MeV is shown in fig. 2a.

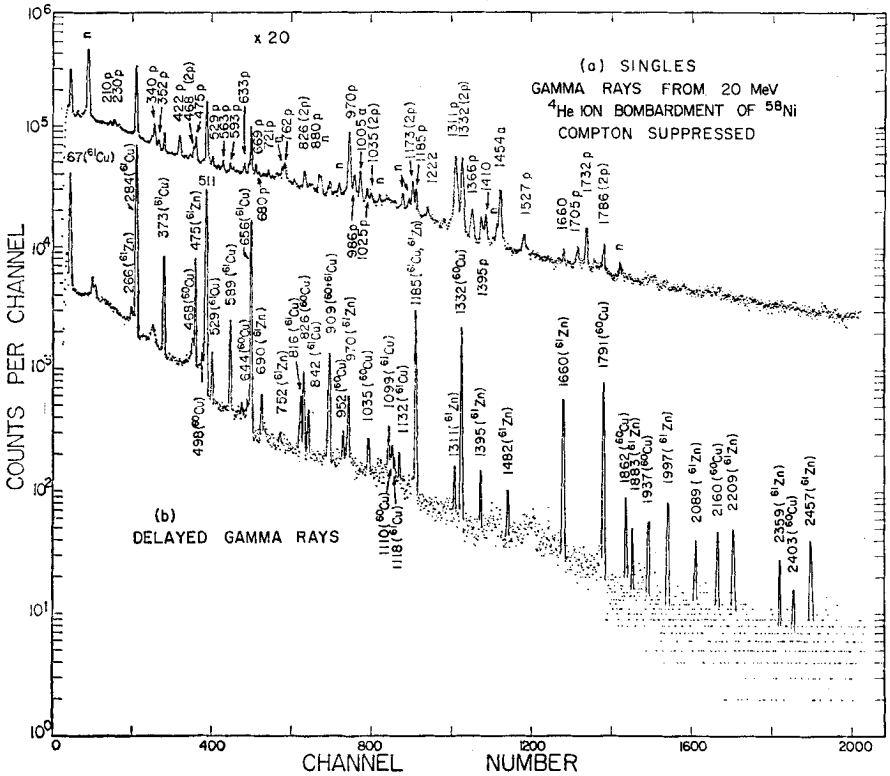

Fig. 2. (a) Compton-suppressed spectrum of the singles prompt and delayed γ-rays from 20.0 MeV $^4He^{++}$ bombardment of ^{58}Ni. Peaks labeled p, 2p, α and n are believed to be associated with the (^{4}He, pγ), (^{4}He, 2pγ), (^{4}He, $\alpha'\gamma$) and (^{4}He, nγ) reactions respectively. (b) Compton-suppressed spectrum of the delayed γ-rays from radioactivity of ^{61}Zn, ^{61}Cu and ^{60}Cu produced in the target.

The lower spectrum (fig. 2b) shows the delayed spectrum from the same experiment. In fig. 2 peaks from the (^{4}He, pγ) reaction are labeled p, from the (^{4}He, 2pγ) reaction are labeled (2p), from the (^{4}He, $\alpha'\gamma$) reaction are labeled α, and those from ^{61}Zn, ^{60}Cu and ^{61}Cu are so labeled. Peaks labeled n were not definitely identified with any known reactions, but presumably are associated with the prompt ^{58}Ni(^{4}He, n) reaction. It is worthwhile to point out that the prompt γ-rays detected at 90° to the beam direction exhibit a noticeable Doppler broadening as it is seen in fig. 2a by comparison with the delayed spectrum. As expected, the increased complexity of the singles spectra

obtained at 15.0 MeV and at higher bombardment energies did not allow the identification of any new γ-rays associated with the decay of levels in ^{61}Cu. In fact only the most prominent γ-rays of those reported in ref. [10]) were observed, although new γ-rays associated with the competing reactions were clearly seen.

3.2. COINCIDENCE pγ CORRELATIONS AT HIGHER ENERGY

As it was shown [10]) in the study of pγ coincidence and singles correlations the results at 12.5 MeV show that the γ-ray yields vary considerably with angle about the beam direction. From that study [10]) it was found that the singles correlations were considerably attenuated over the pγ coincidence correlations. This attenuation is due to the reduction in nuclear spin alignment (change in the population of the magnetic substates) caused by the γ-ray cascades into the levels from the decay of which one observes the correlated transitions.

At the higher projectile energies, for which level yields were determined, it can be assumed that the pγ coincidence correlations are somewhat attenuated over those measured at 12.5 MeV and can be reasonably approximated by those measured in singles at 8.6 MeV. This assumption is expected to be valid because the low-lying levels, from which discrete and characteristic γ-rays can be observed, receive almost their entire population via cascades originating from states in the continuum with a rather limited range of spin values. This assumption was further tested experimentally in one pγ coincidence correlation experiment performed at 20.0 MeV of ^{4}He^{++} bombardment energy. This experiment was performed under the geometry described in subsect. 2.3 above, and it was found from the correlations of the most intense transitions that all measured correlations were somewhat attenuated when compared to the pγ coincidence correlations at 12.5 MeV. The quality of spectra obtained in this 20.0 MeV correlation experiment is seen in fig. 3, where the spectra shown were recorded with the 41 cm^3 Ge(Li) detector for 6 h of coincidence counting for each of the angles of 0°, 30°, 60° and 90° with respect to the beam. These spectra were selected to correspond to a range of proton kinetic energies in the interval of 4.2–5.3 MeV. For this proton energy range both the (^{4}He, pγ) and (^{4}He, 2pγ) reactions occur. The γ-rays labeled p are characteristic of ^{61}Cu and therefore are populated via cascades originating from a region of 9.6–10.8 MeV in ^{61}Cu, from which second proton emission also occurs. The peaks labeled (2p) are associated with the decay of the well known levels [11–14]) of ^{60}Ni.

In the calculation of the yields of levels populated in the (^{4}He, pγ) and (^{4}He, 2pγ) reactions, the angular correlations of the most intense γ-rays from the 20.0 MeV correlation experiment were properly averaged. For the experiments at 18.0 and 22.0 MeV the correction factors for correlation effects obtained from the 20.0 MeV experiment were employed. These correlations are not expected to vary substantially over this small range of bombardment energy. For the weaker γ-rays correction factors from the singles correlations measured in the 8.6 MeV experiments [10]) were employed.

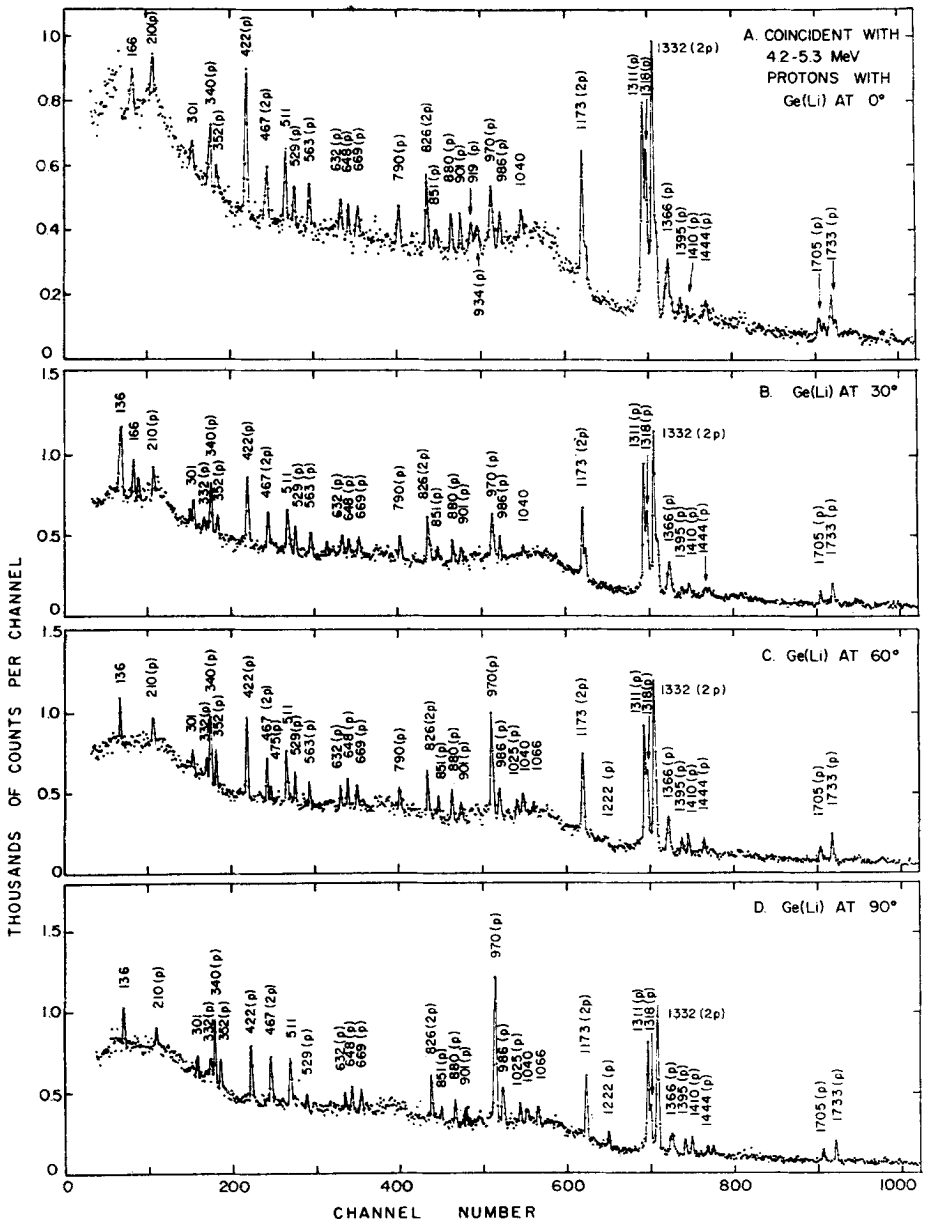

Fig. 3. Spectra of the γ-rays in coincidence with protons with 4.2–5.3 MeV kinetic energy taken with the Ge(Li) detector at the indicated angles with respect to the beam from $^{58}Ni+^{4}He^{++}$ at 20.0 MeV of bombardment energy. Peaks labeled (p) and (2p) are believed to be associated with the de-excitation of levels in ^{61}Cu and ^{60}Ni populated by γ-cascades and proton decay, respectively, from compound states in ^{61}Cu at 9.6–10.8 MeV of excitation.

3.3. PHOTON EMISSION FROM PROTON UNBOUND COMPOUNDS STATES IN ^{61}Cu

In order to measure the relative yields of the γ-rays emitted from the reactions induced by $^4He^{++}$ on ^{58}Ni, the γ-rays in coincidence with the charged particles were measured in two-parameter experiments at bombardment energies of 15.0, 18.0, 20.0 and 22.0 MeV. The relative yields of many γ-rays from the (^{4}He, pγ), (^{4}He, 2pγ) and (^{4}He, pnγ) reactions were determined at each bombardment energy from the pγ

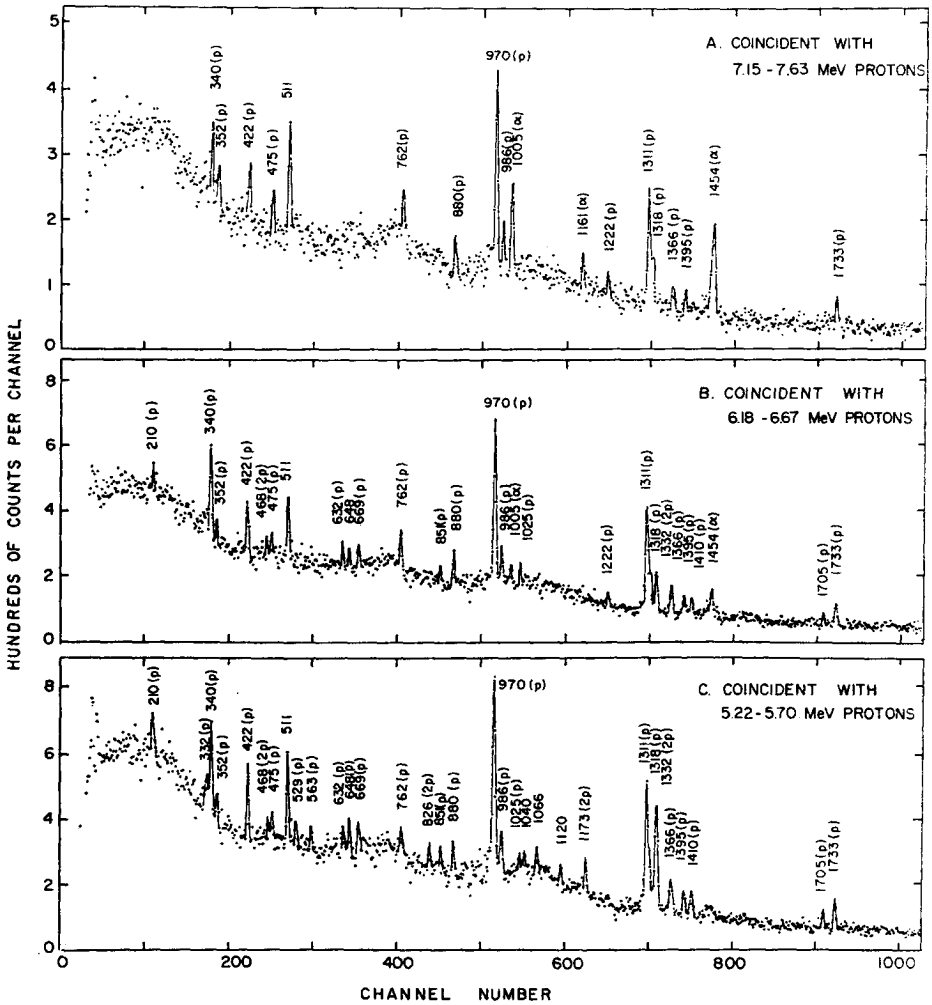

Fig. 4. Spectra of the γ-rays from a 20.0 MeV $^4He^{++}$ bombardment of ^{58}Ni recorded with the 40.8 cm^3 Ge(Li) detector in coincidence with the indicated higher energy regions for the protons detected in the annular Si detector. Peaks labeled (p) and (2p) are believed to be associated with the de-excitation of levels in ^{61}Cu and ^{60}Ni populated by γ-cascades and proton decay, respectively, from compound states in ^{61}Cu at various excitation energies. It is seen that as the proton energy is decreased or the corresponding ^{61}Cu excitation increased, second proton emission begins to occur and for a wide range of energies proton or γ-ray emission occurs from the same compound states.

coincidence information. These γ-ray yields were used in conjunction with the knowledge of the ^{61}Cu, ^{60}Ni and ^{60}Cu level decay schemes to obtain the yields of many individual levels populated in these reactions.

Two-parameter pγ coincidence spectra with good statistics were accumulated for each bombardment energy for a period of 12 h for each energy. The spectra were accumulated in a two-parameter configuration which employed 128 × 2048-channel resolution for the proton and γ-ray axes, respectively.

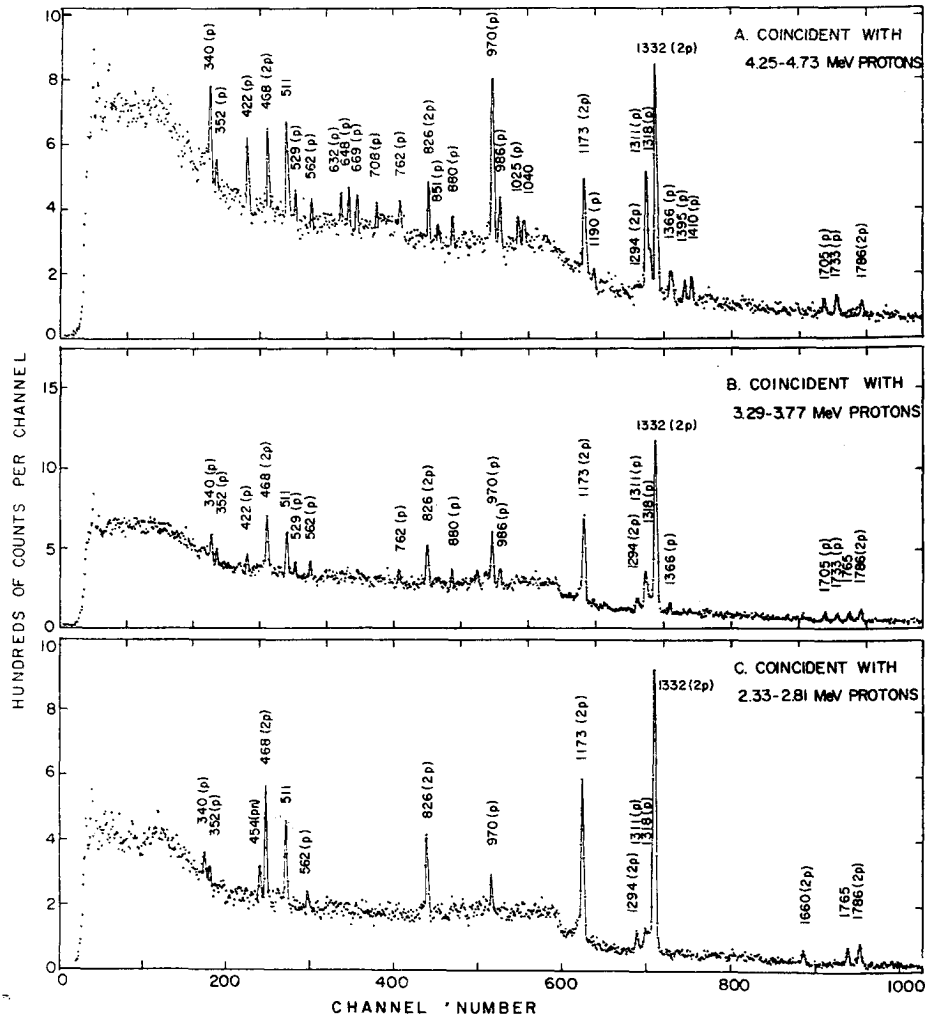

Fig. 5. Spectra of the γ-rays from 20.0 MeV ^{4}He^{++} bombardment of ^{58}Ni recorded with the 40.8 cm^3 Ge(Li) detector in coincidence with the indicated lower energy regions for the protons detected in the annular Si detector. Peaks labeled (p) and (2p) are believed to be associated with the de-excitation of levels in ^{61}Cu and ^{60}Ni populated by γ-cascades and proton decay, respectively, from compound states in ^{61}Cu at various excitation energies. It is seen that as the proton energy is decreased or the corresponding ^{61}Cu excitation increased, second proton emission becomes more prominent than γ-ray emission.

The energy of the proton axis was carefully calibrated with the aid of a mixed α-source of ^{233}U, ^{239}Pu, ^{241}Am and ^{244}Cm. A precision pulser was used to extend the energy calibration to 12.0 MeV. An internal check of the calibration of the proton axis was further provided by the occurrence of two-proton coincidence summing as described below. The energy calibration of the γ-ray axis was achieved by the easily recognizable γ-ray lines from ^{61}Cu and ^{60}Ni in the coincidence spectra.

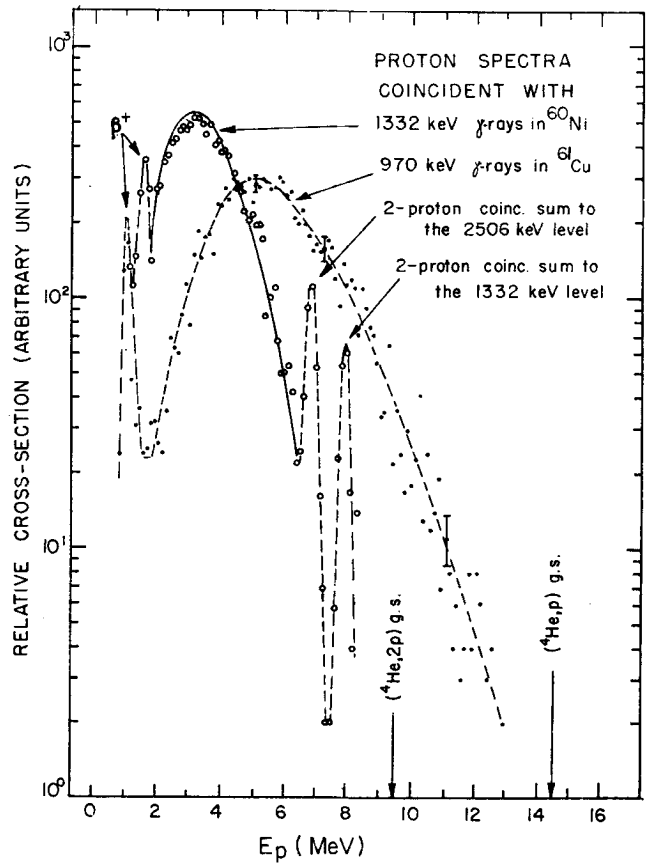

Fig. 6. Spectra of the protons observed in the annular detector in coincidence with the 970.3 and 1332.4 keV peaks in ^{61}Cu and ^{60}Ni, respectively. The spectrum of the protons from the (^{4}He, 2pγ) reaction exhibits two two-proton coincidence summing peaks from the events leading to the population of the 1332.4 and 2505.6 keV levels. Portions of the positon spectra are also seen in the low energy part of each spectrum. Evidence for γ-ray emission from excitation energies as high as 7.7 MeV above the (^{4}He, 2p) threshold is seen, with the most probable emission occurring at 4.5 MeV above the (^{4}He, 2p) threshold.

The two-parameter pγ data were scanned for proton energy intervals of about 480 keV and the γ-ray spectra coincidence with the corresponding proton energies were obtained. In order to minimize illustrations we show in figs. 4 and 5, from the 20.0

MeV experiment only, the γ-ray spectra which are in coincidence with protons in the energy ranges given in the figures and which correspond to the regions of excitation energy in ^{61}Cu of 12.30–12.78, 11.25–11.78, 10.20–10.73, 9.13–9.68, 8.06–8.60, 7.06–7.55 MeV, respectively. These excitation energies in ^{61}Cu, from which γ-ray emission is observed to occur, are as high as 7.8 MeV above the proton separation energy in ^{61}Cu. In figs. 4 and 5 the γ-rays associated with the decay of well known levels in ^{61}Cu are labeled p and those from ^{60}Ni are labeled (2p). As expected, these figures show that the (^{4}He, p) cross section decreases while the (^{4}He, 2p) cross section increases as the proton energy decreases.

Before presenting the quantitative results from these experiments we show in fig. 6 the spectrum of the protons coincident with the 970.3 keV γ-ray in ^{61}Cu and the spectrum coincident with the 1332.4 keV γ-ray in ^{60}Ni. These were obtained from the two-parameter data at the 20.0 MeV bombardment energy by gating on the 970.3 and 1332.4 keV γ-peaks and subtracting the contributions from the underlying Compton events. First, one notices the two-proton coincidence sum peaks which appear in the spectrum coincident with the 1332.4 keV γ-ray. These sum peaks depict the population of the 1332.4 and 2505.6 keV levels in ^{60}Ni and help check the calibration of the proton axis. The energy resolution of these sum peaks represent the system resolution which is $\approx$ 380 keV (FWHM). At the lower energies the contribution to the spectrum due to positons from the decay of ^{60}Cu and ^{61}Zn in the target is also seen. The two spectra in fig. 6 are plotted on an arbitrary scale and represent arbitrary multiples of the respective cumulative yields. The spectrum of the protons from the (^{4}He, pγ) reaction to the 970.3 keV level indicates that the maximum cross section originates from an excitation energy which is 4.5 MeV above the (^{4}He, 2p) threshold and that some γ-cascades originate from excitation energies as high as 7.7 MeV above the (^{4}He, 2p) threshold.

It is clear that the spectra of the protons from the (^{4}He, pγ) reaction uniquely define the excitation energy in ^{61}Cu from which the γ-cascades originate. Due to the indistinguishability of the two protons, however, the spectrum of the protons that lead to the (^{4}He, 2p) reaction does not uniquely determine the excitation energy in ^{61}Cu from which the second proton was emitted. In order to correct the spectra for two-proton coincidence summing, the area of each sum peak was distributed equally to the energy intervals at E_1 and E_2 with $E_1+E_2 = E_{\text{sum}}$ according to the relation $I = I_{\text{sum}}(I_1 I_2)/(\sum I_1 I_2)$, where I_{sum} is the area of the sum peak, and I_1, I_2 are the counts in the intervals at E_1 and E_2. When these spectra are corrected for the small amount of coincidence summing, they represent the sum of the spectra of the first and of the second proton from the (^{4}He, 2p) events that strike the detector at the backward angles. With regard to the shape of the spectrum of the protons from the (^{4}He, p) reaction (dashed line in fig. 6), it should be mentioned that it represents the average overall spectrum to a reasonable approximation. As it is shown in the appendix the angular distribution of the protons emitted from a reaction assumed to proceed via formation and decay of a compound nucleus would result in a few percent increase

of the cross section for the low-energy protons, on the average, relative to that of the higher proton energies when the angle integrated cross sections are calculated. The results presented in this and the following section have not been corrected for this and correspond, therefore, to the differential cross sections at 154° as measured in the present experiments.

3.4. RELATIVE INDEPENDENT YIELDS FOR THE POPULATION OF LEVELS IN ^{61}Cu, ^{60}Ni AND ^{60}Cu FROM ^{58}Ni+^{4}He^{++} INDUCED REACTIONS

The data from the experiments described in subsect. 3.3 were analysed in detail to extract the yield of every identifiable γ-ray in the spectra coincident with the protons of selected energy falling in intervals of about 480 keV. The γ-ray yields were then corrected for detector efficiency and for pγ coincidence correlation effects. From these γ-ray yields it was possible to determine the yields of many individual levels in ^{61}Cu, ^{60}Ni and ^{60}Cu with the aid (i) of the ^{61}Cu and ^{60}Ni level decay schemes [10-13]), and (ii) of a tentative decay scheme for levels in ^{60}Cu shown in fig. 7 and based on present γ-ray information and previous work [14-16]).

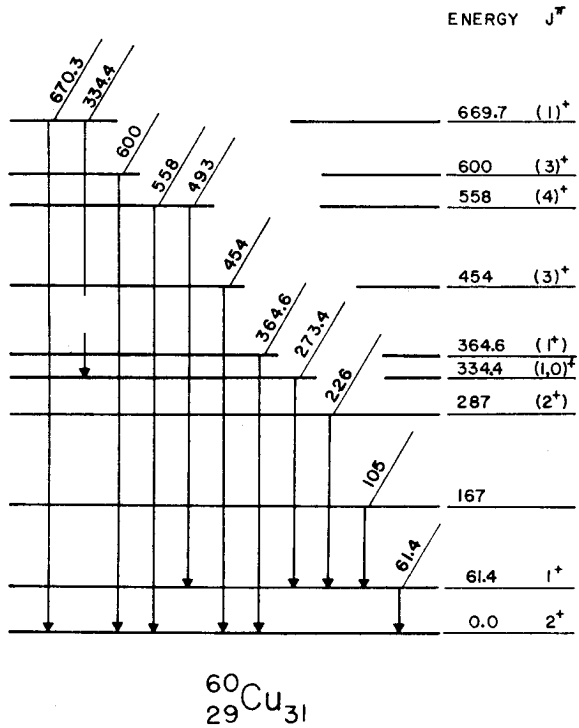

Fig. 7. Tentative scheme for the decay of levels in ^{60}Cu used in the calculation of the ^{58}Ni (^{4}He, pnγ)^{60}Cu reaction yields.

The total independent yield for the population of a level is defined as the yield due to direct population by protons and due to all unobserved γ-ray cascades leading to

that level. For a given bombardment energy the total independent yields for the population of the various levels in ^{61}Cu, as measured in this experiment, are very useful for comparisons and correlations with J^{π} and excitation energy of each level. The independent yields of the levels in ^{60}Ni as determined in these experiments are reported without correction for two-proton coincidence correlation effects and simply correspond to the average of the differential cross sections for detecting either the first or the second proton at $\theta_{ave} = 154°$. Thus, the reported (^{4}He, 2pγ) yields were obtained as one half of the number of protons observed in coincidence with ^{60}Ni γ-rays since in the absence of correlation effects equal numbers of first and second protons are detected with equal probability.

TABLE 1

Summary of the observed fractional independent yields for the levels populated by the ^{58}Ni(^{4}He, pγ) ^{61}Cu reaction at several bombardment energies

Level energy (keV)	J^{π} ref. [10])	% direct population							
		$E_\alpha = 15$ MeV		$E_\alpha = 18$ MeV		$E_\alpha = 20$ MeV		$E_\alpha = 22$ MeV	
475.0	$\frac{1}{2}^-$	2.1	2	1.9	2	0.7	4	0.3	1
970.3	$\frac{5}{2}^-$	10.8	6	11.3	7	7.8	6	3.0	8
(1311.0+2628.4)	($\frac{7}{2}^-$, $\frac{9}{2}^-$)	18.4	20	7.7	40	11.8	30	16.0	30
1394.6	$\frac{5}{2}^-$	3.0	3	2.8	4	2.8	2	2.0	10
1660.5	$\frac{3}{2}^-$	0.70	14						
1732.6	$\frac{7}{2}^-$	7.4	5	7.3	8	8.1	6	5.4	6
1904.5	($\frac{5}{2}^-$)	4.2	3	4.3	8	5.0	4	8.4	8
1932.5	$\frac{3}{2}^-$	1.09	7						
1942.7	$\frac{7}{2}^-$	2.5	2	3.1	9	5.2	11	2.4	4
2088.8	$\frac{1}{2}^-$	3.3	8						
2203.4	($\frac{5}{2}^-$)	1.4	3						
2295.4	$\frac{9}{2}^-$	7.4	7	9.9	9	10.8	8	9.7	10
2336.4	($\frac{9}{2}^-$)	6.2	8	11.5	6	12.1	6	11.3	7
2399.3	$\frac{7}{2}^-$	4.3	3						
2472.9	$\frac{3}{2}^-$	0.6	3						
2583.7	$\frac{5}{2}$	0.8	4	4.6	6	2.4	8	3.8	8
2612.0	$\frac{3}{2}^-$	3.2	10	8.6	5	8.6	7	6.3	12
2720.6	$\frac{9}{2}^+$	2.8	7	4.5	5	7.1	14	3.2	6
2728.4	($\frac{3}{2}$-$\frac{7}{2}$)			1.3	10			3.2	11
2922.9	($\frac{3}{2}$-$\frac{11}{2}$)	1.1	1	1.5	4	3.7	15	2.5	5
3016.1	($\frac{7}{2}$-$\frac{11}{2}$)	7.2	10	7.1	15	6.6	6	2.6	11
3277	($\frac{3}{2}$-$\frac{11}{2}$)	1.6	2	3.4	6	3.9	8	2.5	4
3452	($\frac{3}{2}$-$\frac{11}{2}$)	2.0	10	6.4	9			6.6	8
3546.1	($\frac{1}{2}$-$\frac{9}{2}$)	1.5	5						
3802.0	($\frac{1}{2}$-$\frac{9}{2}$)	3.5	6					4.3	8
3852.1	($\frac{5}{2}$-$\frac{13}{2}$)	1.6							
3950	($\frac{1}{2}$-$\frac{11}{2}$)	1.7		2.8	3	3.4	6	4.5	3

Since only relative yields were measured in this work it is meaningful to define the fractional independent yield for the population of each level in a given reaction product formed at a given bombardment energy. In table 1 we summarize the observed

fractional independent yields for the population of 28 levels in ^{61}Cu formed by the ^{58}Ni(^{4}He, pγ) reaction at 15.0, 18.0, 20.0 and 22.0 MeV of bombardment energy. The first two columns in table 1 give the energy and J^{π} value for each level from ref. [10]).

TABLE 2

Summary of the observed fractional independent yields for the levels populated in the ^{58}Ni(^{4}He, 2pγ)^{60}Ni and ^{58}Ni(^{4}He, pnγ)^{60}Cu reactions are various bombardment energies

Level energy (keV)	J^{π}	% direct population			
		15.0 MeV	18.0 MeV	20.0 MeV	22.0 MeV
^{60}Ni 1332.4	2^+	100	66.4 26	42.2 25	24.7 19
2158.8	2^+		3.1 5	3.5 4	4.5 4
2505.6	4^+		21.8 6	35.7 14	46.4 8
2626.0	3^+		6.0 3	9.7 5	12.1 2
3119	4^+		2.6 5	6.9 6	7.9 11
4156	(5, 6)			2.1 2	4.4 3
^{60}Cu 61.4	$(1)^+$				1.0 4
163	(3, 4, 5)			26.7 28	23.8 6
287	$(2)^+$			11.3 8	10.3 6
364.6	$(0^+, 1^+)$				1.7 2
455	$(3)^+$			29.3 14	24.7 8
558	4^+			23.9 16	20.2 9
597	$(3)^+$			2.6 6	5.4 7
669.7	(0, 1)			5.3 8	12.8 7

TABLE 3

Summary of the observed total independent yields to the ^{58}Ni(^{4}He, pγ), ^{58}Ni(^{4}He, 2pγ) and ^{58}Ni(^{4}He, pnγ) products at 15.0, 18.0, 20.0 and 22.0 MeV ^{4}He^{++} bombardment energies

^{4}He^{++} bombardment energy (MeV)	Percent (^{4}He, pγ)	Percent [a]) (^{4}He, 2pγ)	Percent (^{4}He, pnγ)
15.0	99.8 19	0.2 1	
18.0	87.1 28	12.9 4	
20.0	69.9 29	27.1 8	3.1 1
22.0	55.8 19	33.0 19	11.2 3

[a]) The yield for the population of the ground state by ^{60}Ni may be a significant fraction of the total and this is not observed in the present experiments.

The last four columns give the fractional independent yields of the observed levels for each bombardment energy. These results show that the low-spin levels [10]) ($\leqq \frac{3}{2}$) did not receive any observable population at the higher bombardment energies. In table 2 we summarize the observed fractional independent yields for the population of 6 levels in ^{60}Ni by the (^{4}He, 2p) reaction and 8 levels in ^{60}Cu by the (^{4}He, pn) or (^{4}He, np) reaction at the various bombardment energies. A comparison of the level yields of levels in ^{61}Cu, ^{60}Ni and ^{60}Cu can be made in terms of the total yields to the (^{4}He, pγ), (^{4}He, 2pγ) and (^{4}He, pnγ) reactions summarized in table 3. The total observed yield

for each reaction (with the exception of the direct population of the ground state by proton or neutron decay) is given in table 3 as a percentage for each bombardment energy.

Before the discussion of the various level yield ratios that can be obtained from the results given in tables 1 and 2 we present in the following section the evidence for the dependence of the level yields on excitation energy deposited in the ^{61}Cu compound nucleus for each bombardment energy.

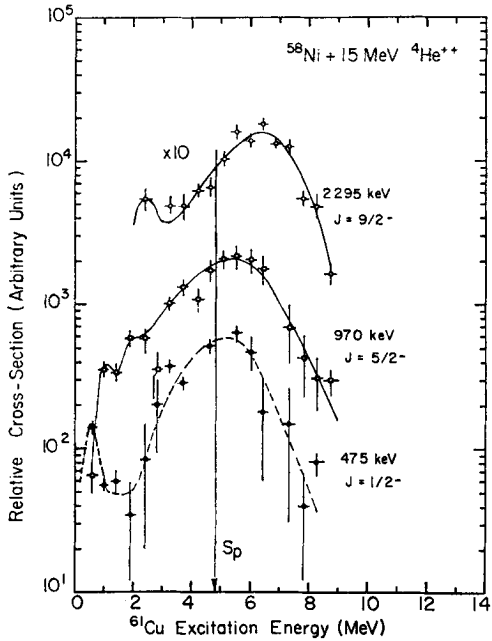

Fig. 8. Variation with excitation energy in ^{61}Cu of the independent yields for the population of the 475.0($\frac{1}{2}^-$), 970.3($\frac{5}{2}^-$) and 2295.4($\frac{9}{2}^-$) keV levels in ^{61}Cu via the ^{58}Ni(^{4}He, pγ) reaction at 15.0 MeV. At this bombardment energy photon emission from proton-unbound states occurs for excitation energies as high as $\approx$ 3.4 MeV above the proton separation energy shown by the line indicated by S_p.

3.5. DEPENDENCE OF THE OBSERVED INDEPENDENT YIELDS OF ^{61}Cu LEVELS ON EXCITATION ENERGY OF THE ^{61}Cu COMPOUND NUCLEUS

The cumulative yields of many levels in ^{61}Cu have been obtained as a function of proton energy and equivalently of excitation energy in ^{61}Cu in the form of curves such as those shown in fig. 6. Many of these levels received considerable population via decay from higher-lying levels through observed γ-transitions. When the yields of the incoming γ-rays to each observed level are subtracted the resulting independent yield curves are in general of poorer statistical quality than those shown in fig. 6.

At low bombardment energy only a small fraction of the yield of each level originates from excitation energies above the proton separation energy in ^{61}Cu($S_p = 4.80$

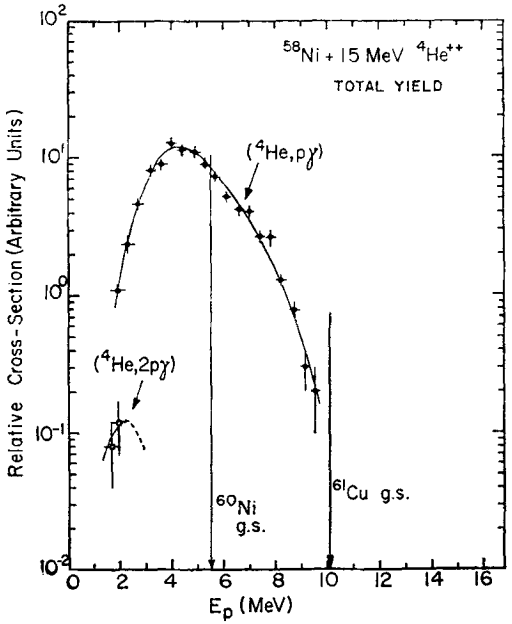

Fig. 9. Variation with observed proton energy of the total ^{58}Ni(^{4}He, pγ) and ^{58}Ni(^{4}He, 2pγ) yields for the 15.0 MeV ^{4}He^{++} bombardment energy.

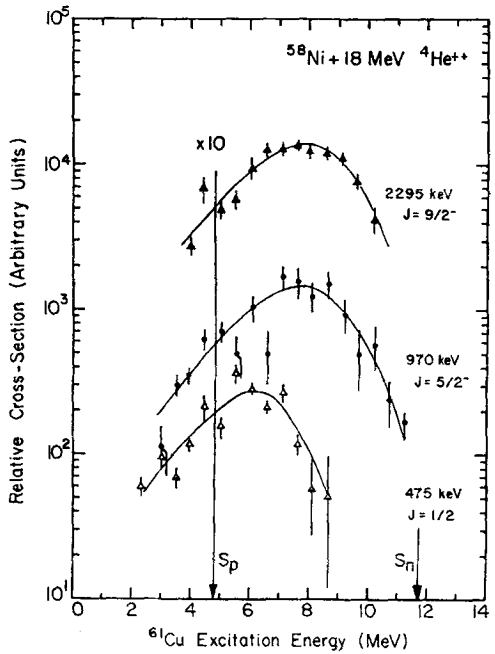

Fig. 10. Independent yields of the levels at 475.0($\frac{1}{2}^-$), 970.3($\frac{5}{2}^-$) and 2295.4($\frac{9}{2}^-$) keV in ^{61}Cu populated via the ^{58}Ni(^{4}He, pγ) reaction as a function of ^{61}Cu excitation energy for a fixed ^{4}He^{++} bombardment energy of 18.0 MeV. It is seen that the largest fraction of the cross section comes from cascades originating from the proton unbound regions and that the maximum yield shifts to higher excitation with increasing spin of the level.

MeV). In fig. 8 we show the variation of the independent yields of only three levels at 475.0($\frac{1}{2}^-$), 970.3($\frac{5}{2}^-$) and 2295.4($\frac{9}{2}^-$) keV with excitation energy in ^{61}Cu obtained in the 15.0 MeV $^4He^{++}$ bombardment of ^{58}Ni. It is seen that for excitation energies corresponding to 3.2 MeV above the proton separation energy the contribution to the level yield becomes negligible. It is interesting to note, however, that the maximum of the yield curves is shifting toward higher excitation with increasing J-value of the level being populated. The total yields for the population of 26 observed levels in ^{61}Cu and the 1332 keV level in ^{60}Ni are shown in fig. 9 as a function of the observed proton

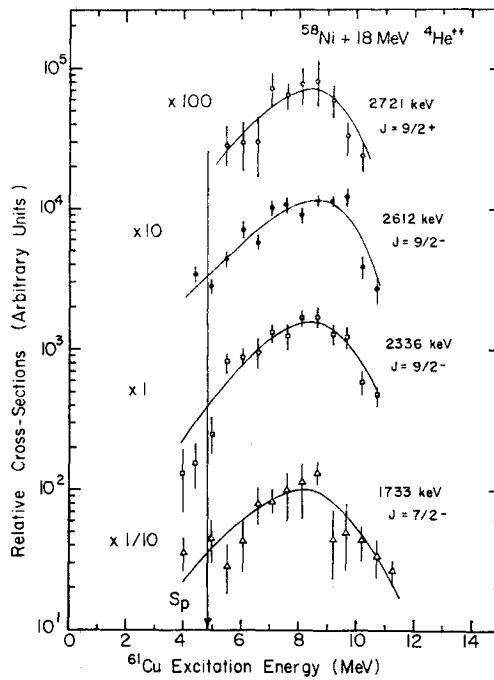

Fig. 11. Independent yields of the levels at 1732.6($\frac{7}{2}^-$), 2336.4($\frac{9}{2}^-$), 2612.0($\frac{9}{2}^-$) and 2720.6($\frac{9}{2}^+$) keV in ^{61}Cu populated via the (^{4}He, pγ) reaction as a function of ^{61}Cu excitation energy for a fixed $^4He^{++}$ bombardment energy of 18.0 MeV. It is seen that most of the cross section comes from cascades that start above the proton separation energy.

energy from 15 MeV $^4He^{++}$ bombardment of ^{58}Ni. Although the yields for the (^{4}He, 2p) reaction are not exactly proportional to the total cross sections due to two-proton correlation effects, such a correction would give an average value that differs by no more than 50 % from the present values when relative cross sections are concerned. It is, therefore, seen that for proton energies allowing the (^{4}He, 2p) reaction to occur, γ-ray emission is predominant for energies of about 3.4 MeV above the proton separation energy. At higher bombardment energies this effect becomes much more pronounced.

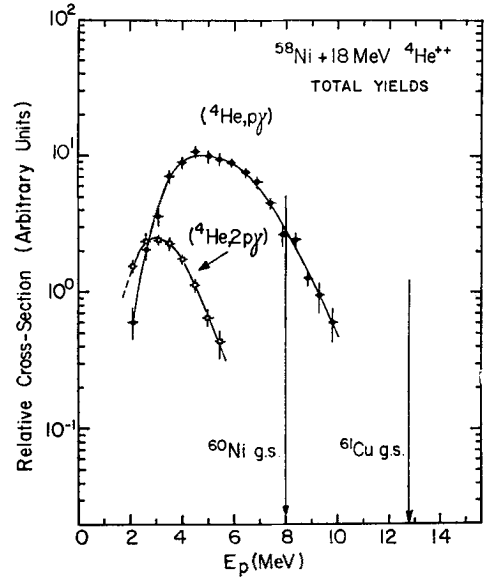

Fig. 12. Total yields for the (^{4}He, pγ) and (^{4}He, 2pγ) reactions as a function of the observed coincident proton energy for 18.0 MeV ^{4}He^{++} bombardment energy. The actual number of protons coincident with ^{60}Ni γ-rays has been divided by 2 to give the relative cross-section shown for the (^{4}He, 2p) reaction.

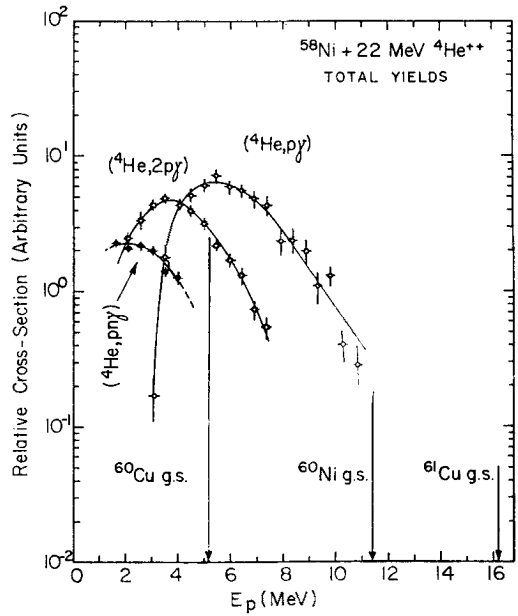

Fig. 13. Total observed yields for the (^{4}He, pγ), (^{4}He, 2pγ) and (^{4}He, pnγ) reactions as a function of the observed coincident proton energy for 22.0 MeV of ^{4}He^{++} bombardment energy. The relative (^{4}He, 2p) yield was obtained by dividing by 2 the number of observed protons in coincidence with ^{60}Ni γ-rays.

When the bombardment energy is raised to 18.0 MeV one observes, as expected, a shift of the yield curves to individual levels toward higher excitation. Thus, in fig. 10 we show the independent yield curves for the population of the 475.0($\frac{1}{2}^-$), 970.3($\frac{5}{2}^-$) and 2295.4($\frac{9}{2}^-$) keV levels as a function of the excitation energy in ^{61}Cu for 18.0 MeV $^4He^{++}$ bombardment energy. By comparison with fig. 8 it is seen that now more than $\approx$ 60 % of each level yield originates from excitation energies above the proton separation energy. There is again a marked shift of the most probable yield toward higher excitation with increasing J-value of the level being populated. For levels with $J \geqq \frac{5}{2}$ the maximum yield comes from excitation energies about 3.5 MeV above the proton separation energy and this is near the proton Coulomb barrier for this system (at this proton energy the $l = 0$ transmission coefficient is 0.144). It is seen, further, that significant photon emission occurs from excitation energies as high as 11.0 MeV, which is just below the neutron separation energy of 11.67 MeV in ^{61}Cu. The marked increase of the yield of the 2295.4 keV $\frac{9}{2}$ level relative to that of the 970.3 keV $\frac{5}{2}^-$ level is worth pointing out. In fig. 11 we show the independent yield curves for the $\frac{7}{2}^-$ level at 1732.6 keV and for the $\frac{9}{2}$ levels at 2336.4, 2612.0 and 2720.6 keV. From these curves it is seen the yields are comparable and that the data do not indicate any noticeable difference in shape. In fig. 12 we show the total observed yield for the (^{4}He, pγ) reaction from 18 levels in ^{61}Cu and for the (^{4}He, 2pγ) reaction from 5 levels in ^{60}Ni as a function of the coincident proton energy for 18.0 MeV of $^4He^{++}$ bombardment energy. It is seen that the largest fraction of the total (^{4}He, p) cross section originates from excitation energies well above the proton separation energy in ^{61}Cu.

When the bombardment energy is raised to 20.0 and 22.0 MeV photon emission in competition with proton emission becomes progressively more pronounced. In fig. 13 we show the total observed yields for the (^{4}He, pγ) reaction from 20 levels in ^{61}Cu and for the (^{4}He, 2pγ) and (^{4}He, pnγ) reactions from six levels in ^{60}Ni and eight levels in ^{60}Cu, respectively, as a function of the observed proton coincident energy for 22.0 MeV of $^4He^{++}$ bombardment energy. These results now clearly indicate that practically the entire (^{4}He, pγ) yield comes from the unbound region via photon emission. It is further seen from fig. 13 that a good fraction of the (^{4}He, pγ) reaction comes from a region of excitation which is also unbound toward neutron emission. In the results of figs. 9, 12 and 13 the number of observed protons from the (^{4}He, 2p) reaction have been divided by 2 to give the total yield shown. Since the events leading to the (^{4}He, pn) or (^{4}He, np) processes are indistinguishable, only the proton yield was plotted in fig. 13.

At the 22.0 MeV of bombardment energy only the levels of high spin ($\frac{7}{2}$, $\frac{9}{2}$ or $\frac{11}{2}$) in ^{61}Cu were seen to receive substantial yields (see table 1). In fig. 14 we show the measured independent yields for the levels at 2295.4($\frac{9}{2}^-$), 2612.0($\frac{9}{2}^-$), 2628.6($\frac{9}{2}^-$), 2336.4($\frac{9}{2}^-$) and 3950($\frac{11}{2}^-$) keV in ^{61}Cu as a function of ^{61}Cu excitation energy. From these plots it is seen that, at 22.0 MeV of bombardment energy, the independent yields of individual levels do not show noticeable difference in shape with excitation energy. The most probable yield for these levels is at $\approx$ 11.5 MeV of excitation or

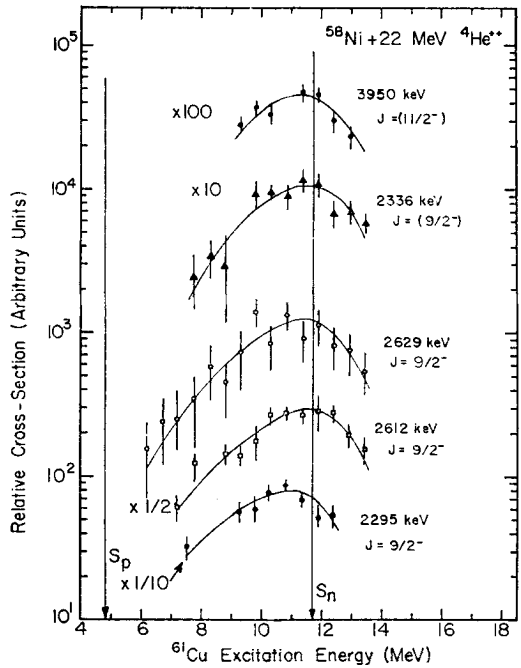

Fig. 14. Measured independent yields for the population of levels at 2295.4 ($\frac{9}{2}^-$), 2612.0($\frac{9}{2}^-$), 2336.4($\frac{9}{2}^-$), 2628.6($\frac{9}{2}^-$) and 3950.0($\frac{11}{2}^-$) keV in ^{61}Cu via the (^{4}He, pγ) reaction as a function of ^{61}Cu excitation energy for a fixed bombardment energy of 22.0 MeV. It is seen that all of the observed cross section comes from cascades that start above the proton separation energy.

TABLE 4

Summary of independent yield ratios for levels in ^{61}Cu observed in the ^{58}Ni(^{4}He, pγ) reaction

Level energy (keV)	J^π value ref. [10])	Independent yield ratio [a])								J^π value deduced from this work [b])
		E_α = 15 MeV		E_α = 18 MeV		E_α = 20 MeV		E_α = 22 MeV		
475.0 [c])	$\frac{1}{2}^-$	0.31	3	0.18	2	0.06	3	0.029	9	$(\frac{1}{2}^-)_1$
970.3 [c])	$\frac{5}{2}^-$	1.60	10	1.06	7	0.68	5	0.29	8	$(\frac{5}{2}^-)_1$
1394.6 [c])	$\frac{5}{2}^-$	0.44	4	0.26	3	0.24	2	0.19	9	$(\frac{5}{2}^-)_2$
1732.6 [c])	$\frac{7}{2}^-$	1.09	7	0.69	8	0.71	5	0.51	6	$(\frac{7}{2}^-)_2$
1904.5 [c])	$(\frac{5}{2}^-)$	0.62	4	0.40	7	0.44	4			$(\frac{5}{2}^-)_3$
1942.7 [c])	$\frac{7}{2}^-$	0.37	3	0.29	8	0.45	10	0.23	4	$(\frac{7}{2}^-)_3$
2295.4 [c])	$\frac{9}{2}^-$	1.09	10	0.93	10	0.94	5	0.92	9	$(\frac{9}{2}^-)_1$
2336.4 [c])	$(\frac{9}{2}^-)$	0.91	12	1.07	5	1.06	5	1.08	7	$(\frac{9}{2}^-)_2$
2583.7	$\frac{5}{2}$			0.43	6	0.21	8	0.36	8	$(\frac{5}{2})_5$
2612.0 [c])	$\frac{9}{2}^-$	0.47	15	0.80	6	0.75	6	0.60	13	$(\frac{9}{2}^-)_3$
2720.6 [c])	$\frac{9}{2}^+$	0.41	10	0.42	5	0.62	12	0.31	6	$(\frac{9}{2}^+)_4$
2922.9 [c])	$(\frac{3}{2}-\frac{11}{2})$	0.16	2	0.14	4	0.32	13	0.24	15	$(\frac{9}{2})_5$, $(\frac{11}{2})$
3016.4	$(\frac{7}{2}-\frac{11}{2})$	1.06	15	0.66	14	0.58	5	0.44	10	$(\frac{7}{2}^-)_4$
3277	$(\frac{3}{2}-\frac{11}{2})$	0.24	3	0.32	6	0.34	7	0.24	4	$(\frac{9}{2})_6$
3452.0 [c])	$(\frac{3}{2}-\frac{11}{2})$	0.29	14	0.60	8			0.63	8	$(\frac{11}{2})_1$, $(\frac{9}{2})$
3802.0	$(\frac{1}{2}-\frac{9}{2})$	0.51	9					0.41	8	$(\frac{9}{2})_7$, $(\frac{7}{2})$
3950.0 [c])	$(\frac{1}{2}-\frac{11}{2})$	0.25	2	0.26	4	0.30	3	0.43	3	$(\frac{11}{2}^-)_2$

[a]) Ratios are computed relative to the weighted average of the yields of the 2295.4 and 2336.4 keV levels known [10]) to be $\frac{9}{2}^-$.

[b]) The subscript outside the parentheses numbers this level with the given J^π value.

[c]) Levels used in the correlation of fig. 15.

$\approx$ 6.7 MeV above the proton separation energy in ^{61}Cu. Considerable yield is also obtained for excitations $\approx$ 2.0 MeV above the neutron separation energy.

3.6. INDEPENDENT YIELD RATIOS FOR LEVELS IN ^{61}Cu FROM THE ^{58}Ni(^{4}He, pγ)^{61}Cu REACTION

The observed fractional independent yields of 28 levels in ^{61}Cu populated via the ^{58}Ni(^{4}He, pγ) reaction were given in table 1. From the present experiments there are 17 levels for which yields were determined for more than one of the bombardment energies employed. It is, therefore, possible to obtain 16 independent yield ratios as

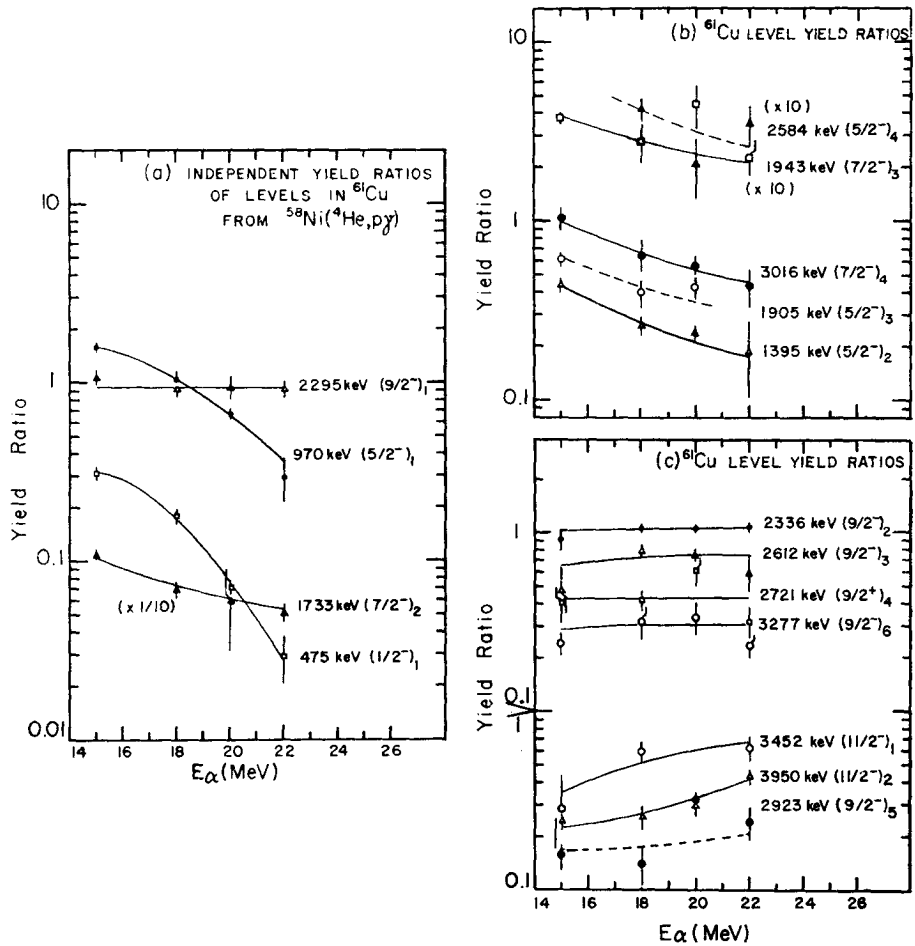

Fig. 15. Ratios of independent yields of levels in ^{61}Cu populated in the ^{58}Ni(^{4}He, pγ) reaction as a function of ^{4}He^{++} bombardment energy. The ratios are relative to the weighted average of the yields of the 2295.4 and 2336.4 keV levels both of which are $\frac{9}{2}^-$. It is seen that the ratios for all levels with $J < \frac{9}{2}$ decrease with increasing bombardment energy, but those with $J = \frac{9}{2}$ remain essentially constant and for those with $J > \frac{9}{2}$ increase.

a function of projectile energy. Such yield ratios are somewhat analogous to the previously reported isomer yield ratios except that here the contributions to the level yields from many observed bound state transitions populating these levels have been subtracted. The independent yield ratios for levels of known J^{π} value are useful in depicting the dependence of the population of levels on the angular momentum content of the compound nuclei involved in the reactions in question.

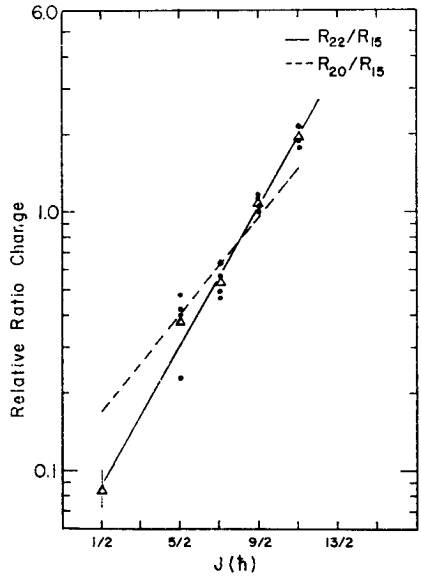

Fig. 16. Empirical correlation of the relative yield ratio change R_{22}/R_{15} from 15 to 22 MeV of $^{4}He^{++}$ bombardment energy with the J-value of the populated levels. The closed circles are the data points for levels summarized in table. 4. The open triangles are the weighted average of each set of points. The solid curve was calculated from the statistical model for the yrast levels in ^{61}Cu. The dashed curve corresponds to the ratio R_{20}/R_{15}.

In order to obtain more meaningful yield ratios from the data of table 1 we have arbitrarily selected to refer all yields relative to the weighted average value of the yields of the 2295.4 and 2336.4 keV levels both of which are known [10]) to be $\frac{9}{2}^{-}$. This choice of reference reduces the errors introduced due to experimental uncertainties in the data points when only one reference level is used. In table 4 we summarize the statistically meaningful yield ratios obtained from the yield data of table 1 for 17 levels in ^{61}Cu. The first two columns in table 4 give the level energy and J^{π} value as established in ref. [10]). Columns 3–6 give the independent yield ratios at 15, 18, 20 and 22 MeV of the $^{4}He^{++}$ bombardment energy. First we note that the J^{π} values given without parentheses in column 2 of table 4 are well established [10]), while those given in parentheses indicate either the most probable value or the possible range of J^{π} values. In fig. 15a we show the variation with bombardment energy of the yield ratios of levels known to be $\frac{1}{2}^{-}$, $\frac{5}{2}^{-}$, $\frac{7}{2}^{-}$ and $\frac{9}{2}^{-}$. These levels, with the exception of the $(\frac{7}{2}^{-})$

level at 1732.6 keV, are yrast levels in ^{61}Cu. In figs. 15b, c we show the ratios for several levels which are known to have or are candidates for J-values of $\frac{7}{2}$, $\frac{9}{2}$ and $\frac{11}{4}$ (see table 4). From the plots of fig. 15 it is apparent that a similarity exists in the shape of the yield ratio curves for states with the same J-value. This result suggests a more quantitative comparison of the changes in these ratios with the J-value the level populated. When one considers the ratio R_{22}/R_{15} of the independent yield ratios for the level (E_i, J_i) at 22.0 MeV relative to that at 15.0 MeV one finds that these ratios for levels of the same J_i are grouped together. In fig. 16 we plot the ratio R_{22}/R_{15} as a function of the J-value of each level. It is seen that R_{22}/R_{15} changes approximately by about a factor of 2 for every increase in J by 1 $\hbar$ unit. With the exception of the points for $J = \frac{5}{2}$ which show a large spread, it is seen that the data points from levels of known J-value are indeed grouped together. It is, therefore, tempting to suggest that an empirical correlation of this form may be useful in limiting the J-value for a number of levels for which yield ratio data were obtained. Thus we find that the levels at 2336.4 and 3277 keV are most likely $\frac{9}{2}$ (see table 4 and fig. 15) since R_{22}/R_{15} for these is near unity. These assignments are summarized in the last column of table 4. Furthermore, we find that the level at 3950.0 and probably at 3452.0 keV are most likely $\frac{11}{2}$, which is consistent with the limits placed in ref. [10]) for the J^π values of these levels. For the levels at 2922.9 and 3806.0 keV the large errors in the yield ratio data allow one to limit J to $\frac{9}{2}$ or $\frac{11}{2}$ and $\frac{7}{2}$ or $\frac{9}{2}$, respectively. When the ratio R_{20}/R_{15} of the yield ratios at 20 and 15 MeV is plotted as a function of J of each level the dashed curve in fig. 16 is obtained. This reduced relative change is expected since at lower bombardment energy the amount of angular momentum imparted to the system is lower and this is reflected on the independent yields.

The values of the independent yield ratios for levels of the same J-value need to be compared next. From the data of table 4 and of fig. 15 we see that for the six $\frac{9}{2}$ levels observed in this work the yield ratios vary considerably. When these ratios are examined as a function of the energy of the level that is being populated one finds an essentially exponential decrease in the ratio with increasing level energy with deviations within the experimental error. The observed overall decrease of the yield ratios with level energy is expected from the statistical theory for the γ-de-excitation due to the reduced phase space available with increasing level energy. Similar trends are observed for the groups of levels with J equal to $\frac{5}{2}$ and $\frac{11}{2}$, but now the scatter of the data points is more pronounced.

3.7. PROTON SPECTRA FROM ^{58}Ni(^{4}He, 2p)^{60}Ni REACTIONS POPULATING INDIVIDUAL ^{60}Ni LEVELS

Spectra of the protons in coincidence with γ-rays known to de-excite well known individual levels in ^{60}Ni were obtained for the 18, 20 and 22 MeV of ^{4}He^{++} bombardment energies. In fig. 17 we show typical spectra of the protons from ^{58}Ni(^{4}He, 2pγ) at 20 MeV recorded in the annular Si detector and which are populating the 1332.4 (2^+), 2158.8(2^+), 2505.6(4^+), 2626.0(3^+), 3119(4^+) and 4165(5, 6) keV levels in ^{60}Ni.

In this experiment either the first or the second proton is detected but not both. Thus the obtained spectra should be symmetrical about a proton energy value determined by the reaction energetics, in view of the fact that, apart from the kinematic correction, the sum of the two proton energies populating a given level should equal a constant. This is seen in the results shown in fig. 17 in which the spectra shown have been corrected for two-proton coincidence summing. The spectra of fig. 17 are given with respect to the observed proton energy in the laboratory coordinates and therefore are

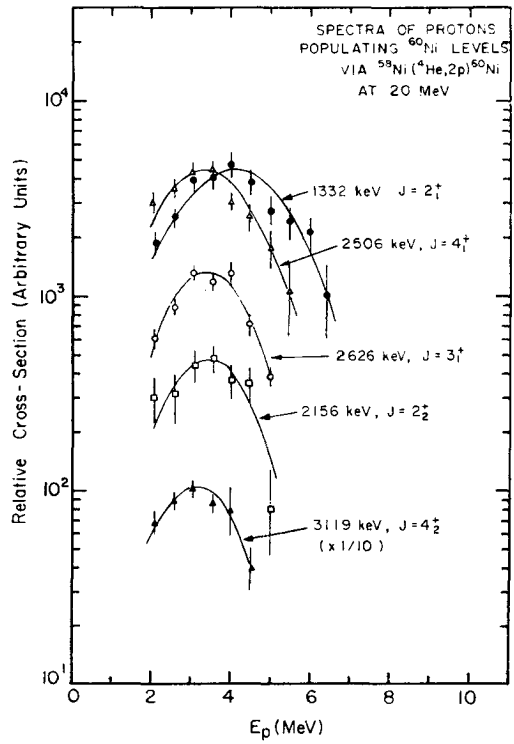

Fig. 17. Spectra of the protons observed to populated individual levels in ^{60}Ni via the ^{58}Ni(^{4}He, 2p) reaction at 20.0 MeV of bombardment energy.

subject to a small kinematic broadening due to the fact that the angle of emission of one of the two protons is not observed. The mid position of the spectra of fig. 17 to each level in ^{60}Ni follows the kinematics of the ^{58}Ni(^{4}He, 2p)^{60}Ni reaction according to which the lower lying levels are populated by protons of higher kinetic energy. From the data of fig. 17 and the yields of table 2 it is seen that the 4^+ level at 2505.6 keV receives a large yield despite the fact that it is not energetically favored when compared to the 2^+ level at 1332.4 keV.

In order to demonstrate the variation of the relative yields for the levels in ^{60}Ni populated in the (^{4}He, 2p) reaction we plot in fig. 18 the independent relative level

yields with respect to the yield of the 2^+ 1332.4 keV level in ^{60}Ni. It is seen that the yield ratios increase markedly with increasing bombardment energy. This result reflects in part the fact that with increasing bombardment energy the proton decay to the higher-lying levels from many compound states in ^{61}Cu is subject to reduced Coulomb barrier restrictions while centrifugal barrier restrictions are energy independent.

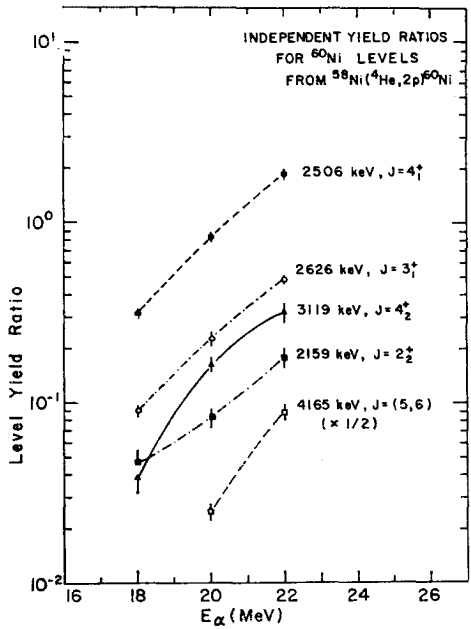

Fig. 18. Independent yields for individual levels in ^{60}Ni populated via ^{58}Ni(^{4}He, 2p) relative to the yield of the 1332.4 keV (2^+) level.

4. Discussion and conclusions

The results reported in this work clearly indicate that γ-ray emission occurs favorably over proton or neutron emission from compound states lying as high as ≈ 8 MeV above the proton separation energy or ≈ 1.5 MeV above the neutron separation energy in the ^{61}Cu compound nucleus. The dependence of the total (^{4}He, pγ) cross section on the excitation energy for the ^{61}Cu compound nucleus was indirectly depicted for various bombardment energies in figs. 9, 12 and 13. We summarize these results in fig. 19, where we plot the ^{61}Cu yields from all observed levels, corrected for angular distribution effects (see appendix) as a function of the excitation energy of the ^{61}Cu compound nucleus for the four bombardment energies of 15, 18, 20 and 22 MeV. For these bombardment energies ^{4}He^{++} are "good compound nucleus projectiles". At higher bombardment energies (> 30 MeV) pre-equilibrium evaporation becomes important [17]). The present experiments were carried out with a beam spread of 250–400 keV for the experiments from 15 through 22 MeV which is sufficiently

wide to average over the fluctuations in cross section. The results reported in this work are in agreement with the predictions of the compound statistical model. A detailed theory based on the compound statistical model utilizing basically the formalism of refs. [1, 2]) and suitable for calculating the quantities measured in the present experiments has been formulated. Since the detailed evaluation of the parameters entering in the theory deserves extensive comparison with the present data, we will report the results of the calculations in more detail in another communication. Here we discuss some of the essential features related to the trends predicted by the statistical model that are pertinent in the interpretation of the present experimental data.

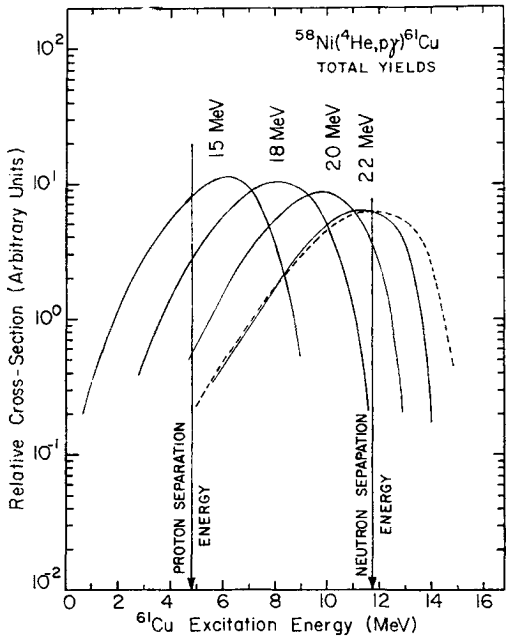

Fig. 19. Relative cross sections (solid curves) for the population of levels in ^{61}Cu via the (^{4}He, pγ) reaction with excitation energy of the ^{61}Cu compound nucleus for various bombardment energies. The dashed line is the calculated initial distribution for states of all angular momenta in ^{61}Cu following the first proton emission in ^{58}Ni+^{4}He^{++} at 22 MeV.

First we mention that using eqs. (2) or (3) of ref. [1]) one can calculate $\sigma_{\text{comp}}(J, J_c)$ which gives the ^{62}Zn compound nucleus spin distribution for an excitation energy U. Using this relationship and optical model transmission coefficients calculated with aid of OPTIM [18]), an optical-model code, we obtained the root-mean-square values of 5.56, 6.74, 7.43 and 8.05 $\hbar$ units for the distributions from the 15, 18, 20 and 22 MeV ^{4}He^{++} bombardments of ^{58}Ni. Using the notation of ref. [1]) we can write the

relative population of levels in ^{61}Cu as

$$P(E_p, J_p) = \sum_{J_c} \frac{\sigma_{comp}(U, J_c)}{\sum_i \Gamma_i(U, J_c)} R_p(UJ_c; E_p J_p), \quad (1)$$

where $R_p(UJ_c; E_p J_p)$ is the proton emission rate from an initial state (U, J_c) in ^{62}Zn to a final state (E_p, J_p) in ^{61}Cu given by eq. (9) of ref. [1]) and $\Gamma_i(U, J_c)$ is the emission function given by eq. (1) of ref. [1]). Expression (1) gives the population of the compound ^{61}Cu states, the decay of which by proton or γ-ray emission was investigated in the present experiments. The population distribution $P(E_p, J_p)$ in ^{61}Cu was evaluated, using a Fermi gas level density expression [see eq. (24) of ref. [1])] with $a = \frac{1}{10}A$ and a rigid-body moment of inertia, for 15, 18, 20 and 22 MeV of bombardment energy. Further, the quantity $Q(E_p) \equiv \sum_{J_p} P(E_p, J_p)$ gives the relative population of compound states of all spins in ^{61}Cu prior to γ-ray or particle emission. The γ-ray cascades to all bound levels in ^{61}Cu are not expected to alter drastically the distribution $Q(E_p)$. If this expectation is correct then the measured distributions of total yields in ^{61}Cu with excitation energy shown as solid lines in fig. 19 should follow the shape of $Q(E_p)$. The dashed curve in fig. 19 gives the $Q(E_p)$ distribution for the 22 MeV bombardment energy. Comparison of this $Q(E_p)$ curve with the measured yield curve for (^{4}He, pγ) at 22 MeV shows that the experimental curve has a maximum at somewhat lower energy and that at high excitation the yield curve is below the initial population. The preferential proton decay, however, from the high excitation energies accounts for part of the difference. The results of fig. 19 for 15, 18 and 20 MeV, however, are well reproduced by the theoretical calculation.

The calculated distribution $P(E_p, J_p)$ can be used to estimate the root-mean-square value $\sqrt{\bar{J}^2}$ for the states in the compound ^{61}Cu nucleus. For reasonable values of the moment of inertia between 0.5–1.0 of the rigid rotor value we obtain an approximate reduction of $\sqrt{\bar{J}^2}$ by about 0.7 $\hbar$ units. The persisting emission of photons from higher excitations as the bombardment energy is increased, is accounted for by the increased angular momentum deposited in the compound ^{61}Cu nucleus and by the lack of high angular momentum states in the even ^{60}Ni nucleus to which proton decay can occur without severe centrifugal barrier restrictions.

The observed fractional independent yields of levels in ^{61}Cu are worth considering next. First we point out that the yields given in table 1 show that at the high bombardment energies there is a strong preference for population of the $\frac{9}{2}$ and $\frac{11}{2}$ states. No other $J > \frac{11}{2}$ states have been thus far identified in ^{61}Cu. A substantial number of lower spin states have been identified [10]) in the excitation energy range of 2.30–3.95 MeV where the $\frac{9}{2}$ and $\frac{11}{2}$ states were observed to receive significant population. Although the present experimental sensitivity does not allow us to place a very low upper limit for the population of $J < \frac{5}{2}$ states ($\approx \frac{1}{10}$ of the average observed intensity) the observed level yield trends from the 18 MeV data suggest that the yield of such states rapidly decreases with excitation energy of each bound level. It is possible that

a good portion of the independent yield of the low-lying spin states comes from indirect population by decay of a larger number of higher-lying but weakly populated low-spin states. It may be of interest to point out that the change of the level yield ratios with bombardment energy shown in fig. 16 are predicted by the statistical-model calculations. In fact the solid line in fig. 16 was calculated from the energy variation of the yields of the yrast levels in ^{61}Cu.

Whereas the shape of the level yield curves with excitation energy is expected to be rather insensitive to the assumed value for the moment of inertia in the level density expression, (dashed line in fig. 19) it was found quite sensitive to the level density parameter a used. The total independent yield distributions, however, are quite sensitive to the assumed moment of inertia which defines the $P(E_p, J_p)$ distribution of eq. (1).

Finally, we mention that from these experiments the relative (^{4}He, pγ) and (^{4}He, 2pγ) yields can be used in conjunction with the statistical model to extract the relative widths for γ-ray and proton emission as a function of excitation energy and J of the emitting state.

We wish to express our thanks to Mr. John Hood and the personnel of the Washington University Cyclotron for the continued cooperation during the course of these experiments. The cooperation of the staff of the Washington University computing facilities is appreciated.

Appendix

CORRECTIONS DUE TO ANGULAR DEPENDENCE OF THE DIFFERENTIAL CROSS SECTION FOR THE (^{4}He, p) REACTION

The spectra of the protons from the (^{4}He, p) reaction (figs. 9, 12 and 13) have a shape which is to a reasonable approximation typical of the averaged spectrum. It is known that particles emitted from compound-nucleus reactions exhibit an angular distribution about the beam direction. By making a number of approximations, Ericson and Strutinskii [19]) derived the following simple expression for the angular dependence of the differential cross-section, namely,

$$\frac{\mathrm{d}^2\sigma_{ab}(\varepsilon_b, \theta)}{\mathrm{d}\varepsilon_b \, \mathrm{d}\Omega_b} = \text{const}\left\{1 + \tfrac{1}{12}\frac{\langle l_a^2(\varepsilon_a)\rangle\langle l_b^2(\varepsilon_b)\rangle}{\sigma^4} P_2(\cos\theta)\right\},$$

where $\langle l_a^2(\varepsilon_a)\rangle$ and $\langle l_b^2(\varepsilon_b)\rangle$ are the mean-square-orbital angular momenta of the projectile and emitted particle, respectively; and σ is the spin cut-off parameter in expression for the level density. The mean-square orbital momenta are given by the relation

$$\langle l^2(\varepsilon)\rangle = \frac{\sum_0^\infty l^3 T_l(\varepsilon)}{\sum_0^\infty l T_l(\varepsilon)},$$

where $T_l(\varepsilon)$ are the optical model transmission coefficients. The validity of this approximation has been examined by Vonach and Huizenga [20]). Using optical model transmission coefficients [18]), and rigid rotor moment of inertia corresponding to $\sigma = 3.6$ for this system we calculate that the maximum correction to obtain the angle integrated spectrum corresponds to a 14 % increase of the number of the 3 MeV protons relative to the 11 MeV protons in the 22 MeV $^4He^{++}$ bombardment. The spectra shown in fig. 19 (solid lines) have been corrected for the angular distribution effect.

References

1) D. G. Sarantites and B. D. Pate, Nucl. Phys. **A93** (1967) 545
2) D. G. Sarantites, Nucl. Phys. **A93** (1967) 567, 576
3) J. R. Grover and J. Gilat, Phys. Rev. **157** (1967) 802, 814
4) J. M. Alexander and G. N. Simonoff, Phys. Rev. **133** (1964) B93
5) D. C. Williams and T. D. Thomas, Nucl. Phys. **A92** (1967) 1;
T. D. Thomas, Nucl. Phys. **53** (1964) 577
6) J. F. Mollenauer, Phys. Rev. **127** (1962) 867
7) J. O. Newton, F. S. Stephens, R. M. Diamond, W. H. Kelly and D. Ward, Nucl. Phys. **A141** (1970) 631
8) B. L. Cohen, J. H. Degnan, C. L. Fink, G. R. Rao and R. Balasubramanian, Phys. Rev. Lett. **26** (1971) 23
9) D. G. Sarantites and W. G. Winn, Nucl. Phys. **A155** (1970) 257
10) E. J. Hoffman and D. G. Sarantites, Nucl. Phys., **A173** (1971) 146
11) E. J. Hoffman and D. G. Sarantites, Phys. Rev. **181** (1969) 1597
12) F. Rauch, D. M. Van Patter and P. F. Hinrichsen, Nucl. Phys. **A124** (1969) 145
13) D. M. Van Patter, H. L. Scott and C. Moazed, Communication 4.37 Int. Conf. on properties of nuclear states, Montreal, Aug. 1969, p. 124
14) E. J. Hoffman and D. G. Sarantites, Phys. Rev. **177** (1969) 1640
15) J. H. Young and J. Papaport, Phys. Lett. **26B** (1968) 143
16) L. Birstein, C. Drory, A. A. Jaffe and Y. Zioni, Nucl. Phys. **A97** (1967) 203
17) M. Blann and F. M. Lanzafame, Nucl. Phys. **A142** (1970) 559
18) OPTIM, an optical model program written by D. Zurstadt, Univ. of Colorado Cyclotron Report No. 6835, modified by G. R. Siegel (1970)
19) T. Ericson and V. M. Strutinskii, Nucl. Phys. **8** (1958) 284
20) K. H. Vonach and J. R. Huizenga, Phys. Rev. **149** (1966) 844